

KTI LETTER REPORT

**THE USE OF POLYSTYRENE MICROSPHERES AS TRACER SURROGATES FOR
INORGANIC GROUNDWATER COLLOIDS**

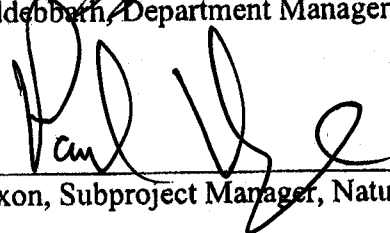
April 2002

Preparation:


P.W. Reimus, Principal Investigator, Saturated Zone Department 04-03-02
Date

Approval:


A.A. Eddebbah, Department Manager, Saturated Zone 04-02-02
Date


P.R. Dixon, Subproject Manager, Natural Systems 4-4-02
Date

Reviewed by:


Ming Zhu, License Application Project 4/4/02
Date

TABLE OF CONTENTS

	Page
LIST OF FIGURES	iii
LIST OF TABLES	iv
ACRONYMS AND ABBREVIATIONS	v
1. THE USE OF POLYSTYRENE MICROSPHERES AS TRACER SURROGATES FOR INORGANIC GROUND WATER COLLOIDS	1
1.1 CML MICROSPHERE AND SILICA TRANSPORT IN FRACTURED VOLCANIC ROCKS	3
1.2 CML MICROSPHERE AND SILICA TRANSPORT IN SATURATED ALLUVIUM	14
2. CONCLUSIONS	21
3. INPUTS AND REFERENCES	22
3.1 DOCUMENTS CITED	22
3.2 CODES, STANDARDS, REGULATIONS, AND PROCEDURES	22

LIST OF FIGURES

	Page
1. Normalized Concentrations of 330-nm Diameter CML Microspheres, 100-nm Diameter Silica Spheres, and Iodide in Fractured Core from ER-20-6#1 at 2407 ft.....	8
2. Normalized Concentrations of 330-nm Diameter CML Microspheres, 100-nm Diameter Silica Spheres, and Iodide in Fractured Core from PM-2 at 7032 ft @10mL/hr.....	9
3. Normalized Concentrations of 330-nm Diameter CML Microspheres, 100-nm Diameter Silica Spheres, and Iodide in Fractured Core from PM-2 at 7032 ft @2.5 mL/hr.....	10
4. Normalized Concentrations of 330-nm Diameter CML Microspheres, 100-nm Diameter Silica Spheres, and Iodide in Fractured Core from PM-2 at 7032 ft, Vertical Core Orientation	11
5. Normalized Concentrations of 330-nm Diameter CML Microspheres, 100-nm Diameter Silica Spheres, and Iodide in Fractured Core from PM-2 at 7032 ft, Horizontal Core Orientation	12
6. Log Normalized Concentrations of 330-nm Diameter CML Microspheres, 100-nm Diameter Silica Spheres, and Bromide in Alluvium-Packed Column A	16
7. Log Normalized Concentrations of 330-nm Diameter CML Microspheres, 100-nm Diameter Silica Spheres, and Bromide in Alluvium-Packed Column B	17
8. Log Normalized Concentrations of 330-nm Diameter CML Microspheres, 100-nm Diameter Silica Spheres, and Bromide in Second Experiment in Alluvium-Packed Column A.....	20
9. Log Normalized Concentrations of 330-nm Diameter CML Microspheres, 100-nm Diameter Silica Spheres, and Bromide in Second Experiment in Alluvium-Packed Column B	21

LIST OF TABLES

	Page
1. Comparison of Properties of CML Microspheres and Inorganic Groundwater Colloids	2
2. Properties of CML Microspheres and Silica Spheres Used in Experiments	3
3. Properties of the Fractured Cores Used in the Colloid Transport Experiments: Physical Characteristics	4
4. Properties of the Fractured Cores Used in the Colloid Transport Experiments: X-ray Diffraction Results (wt %)	4
5. Properties of the Fractured Cores Used in the Colloid Transport Experiments: Lithologic Descriptions	5
6. Chemical Composition of U-20WW Groundwater	5
7. Summary of Experimental Conditions in the Fractured Core Tests	6
8. Model Parameters from RELAP Fits of Tracer Breakthrough Curves in Experiments in Fractured Core from Borehole PM-2	12
9. Characteristic Diffusion and Settling Lengths (L_D and L_S) for the CML Microspheres and Silica Spheres in the Four Experiments in the Fractured Core from Borehole PM-2	13
10. Estimates of Filtration Rate Constants and Detachment Rate Constants for CML Microspheres and Silica Colloids in Columns Packed with Alluvium	19

ACRONYMS AND ABBREVIATIONS

ATC	Alluvial Testing Complex
CML	Carboxylate-modified latex
IDC	Interfacial Dynamics Corp.

1. THE USE OF POLYSTYRENE MICROSPHERES AS TRACER SURROGATES FOR INORGANIC GROUND WATER COLLOIDS

Carboxylate-modified latex (CML) polystyrene microspheres were used as colloid tracers in the multiple-tracer tests in both the Bullfrog Tuff and the Prow Pass Tuff at the C-wells complex. CML microspheres were also used in one of the three single-well tracer tests in the saturated alluvium at NC-EWDP-19D1, and they will be used in at least one cross-hole tracer test at the Alluvial Testing Complex (ATC). CML microspheres were selected as colloid tracers in these field tests because they are very monodisperse (i.e., they have a very narrow range of diameters) and they can be obtained with various fluorescent dyes incorporated into their polymer matrix, which allows them both to be detected at very low concentrations and to be discriminated from natural, nonfluorescing colloids using methods such as epifluorescent microscopy and flow cytometry. Flow cytometry (Steinkamp et al. 1991) has been used as the microsphere detection and quantification method for all field tracer tests in which microspheres have been used as tracers. This technique allows quantification at microsphere concentrations as low as 100/mL in the presence of natural background colloid concentrations that are 2 to 4 orders of magnitude higher. These levels of detection and discrimination are currently not attainable using any other type of colloid tracer except perhaps viruses/bacteriophages (Bales et al. 1989).

CML microspheres were chosen over other types of polystyrene latex microspheres as field colloid tracers for two reasons: (1) they have surface carboxyl groups that give them a negative surface charge at pH greater than about 5; and (2) they have relatively hydrophilic surfaces compared to other types of polystyrene microspheres (Wan and Wilson 1994). These properties are consistent with those of natural inorganic groundwater colloids. The hydrophilic surfaces of CML microspheres are the result of their matrix being comprised of a copolymer of styrene and acrylic acid rather than pure styrene. This copolymer gives the CML microspheres a higher surface density of carboxyl groups and also a significantly higher degree of surface hydrophilicity than other types of polystyrene microspheres, including "carboxylated" spheres that consist of a pure polystyrene matrix. Fluorescent dyes are generally incorporated into the microspheres by swelling the spheres in an organic solvent containing the dye and then washing the spheres in an aqueous solution to expel the solvent and shrink them back to their original size. Dye molecules tend to remain behind in the spheres because of their affinity for the organic matrix.

The CML microspheres used in Yucca Mountain field tracer tests have all been purchased from Interfacial Dynamics Corp. (IDC) because IDC uses a surfactant-free synthesis process that does not require microspheres to be cleaned (by dialysis or centrifugation) to remove trace levels of surfactant before they are used in tests. Small levels of surfactants can greatly affect microsphere surface characteristics, resulting in inconsistency and irreproducibility of their transport behavior.

CML microspheres have properties that make them the best choice among synthetic polystyrene microspheres as reasonable surrogates for inorganic colloids. Table 1 provides a comparison of properties of CML microspheres and groundwater colloids. It is clear that although the two types of colloids differ in density, shape, and specific surface chemistry, they have common surface charge and hydrophilicity.

Table 1. Comparison of Properties of CML Microspheres and Inorganic Groundwater Colloids

Property	CML Microspheres	Inorganic Groundwater Colloids
Size	Monodisperse but greater than 200-nm diameter to ensure good fluorescence detection	Polydisperse, ranging from < 50 nm to > 1 μm
Density	1.055 g/cm ³	2.0–2.6 g/cm ³
Shape	Spherical	Variable, including polygons, rods, and platelets
Surface Chemistry	Carboxyl groups with many polymer chains extending into solution	Variable, with silicate, iron oxide, aluminum oxide, manganese oxide, and other surface groups possible
Zeta potential	-30 mV or less in low ionic strength water at neutral pH	-30 mV or less in low ionic strength water at neutral pH
Hydrophobicity	Hydrophilic	Hydrophilic
pH at point of zero charge	~5.0	Variable, but generally less than 5 or 6

To address the suitability of using CML microspheres as surrogates for natural inorganic colloids, a limited number of laboratory experiments were conducted in which the transport behavior of CML microspheres was compared with that of silica spheres in both saturated volcanic tuff fractures and saturated alluvium-packed columns. All tests were conducted using the same CML microspheres (330-nm diameter spheres from IDC dyed with a fluorescent yellow-green dye) and silica spheres (100-nm diameter spheres from Nissan Chemical). Table 2 provides further information on the two colloid tracers. Silica spheres were used for the comparison studies because previous testing had indicated that silica spheres transport with much less attenuation through fractures than clay (montmorillonite) colloids (Reimus et al. 2001). Thus, if CML microspheres were shown to transport conservatively (with minimal attenuation) relative to silica spheres, they would be expected to transport even more conservatively relative to clay colloids.

The 330-nm CML microspheres were selected to be representative of microspheres with diameters ranging from about 250 to 500 nm, which represents a practical size range that can be used in field tests (detection-limited at the small end, and cost-limited at the large end). Microspheres at the upper end of this size range will settle about twice as fast and diffuse about one-third slower than 330-nm diameter spheres, and microspheres at the lower end of this range will settle about half as fast and diffuse about one-fourth faster than 330-nm diameter spheres. Thus, the entire CML microsphere size range from 250 to 500 nm (diameter) will both settle slower and diffuse slower than 100-nm silica colloids. These characteristics (slower settling and diffusion) are both desirable from the standpoint of reducing the number of colloid collisions with aquifer surfaces. Thus, if electrochemical interactions between colloids and aquifer surfaces are similar for both colloids (as suggested by the similar zeta potentials of the colloids in Table 2), the microspheres would be expected to transport conservatively relative to the silica.

Table 2. Properties of CML Microspheres and Silica Spheres Used in Experiments

Property	CML Microspheres	Silica Spheres
Particle Diameter (nm)	330 ± 11	100
% Solids (g/100g) ⁽¹⁾	2 ± 0.1	40.7
Stock Conc. (number/mL) ⁽¹⁾	1 × 10 ¹²	3.8 × 10 ¹⁴
Density (g/cm ³)	1.055	2.65
Dye Excitation/Emission Wavelengths (nm)	505/515	No Dye
Diffusion Coefficient (cm ² /s) ⁽²⁾	1.34 × 10 ⁻⁸	4.43 × 10 ⁻⁸
Specific Surface Area (cm ² /g)	1.7 × 10 ⁵	2.3 × 10 ⁵
Surface Charge (meq/g) ⁽⁴⁾	0.08	NM ⁽³⁾
Zeta Potential in U-20WW Water (mV) ⁽⁵⁾	-42.7 ± 9.1	-41.2 ± 4.1
Zeta Potential in NC-EWDP-19D1 Water (mV)	NM	-45.15 ± 2.9

- NOTES: ⁽¹⁾ Manufacturer's stock solution in deionized water; solutions used in experiments were diluted in ground water to several orders of magnitude below these concentrations.
- ⁽²⁾ Calculated using the Stokes-Einstein equation, $D = kT/(6\pi\mu R)$, where k = Boltzmann's constant (1.38×10^{-16} ergs/K), T = temperature ($^{\circ}$ K), μ = fluid viscosity (g/cm-s), and R = colloid radius (cm).
- ⁽³⁾ NM = not measured.
- ⁽⁴⁾ Value reported by the manufacturer (Interfacial Dynamics Corp.).
- ⁽⁵⁾ The zeta potential is the potential measured at the "surface of shear" near the colloid surface in solution. The surface of shear occurs where water molecules transition from being immobile to being mobile relative to the colloid surface when the colloid moves under the influence of an imposed potential gradient in an otherwise static solution. The zeta potential is generally considered to be the best measure of the strength of electrostatic interactions between colloids or between colloids and surfaces in solution (Hiemenz 1986).

1.1 CML MICROSPHERE AND SILICA TRANSPORT IN FRACTURED VOLCANIC ROCKS

Testing in fractured volcanic rock was conducted in two different fractured cores from Pahute Mesa at Nevada Test Site, with the majority of the testing being done in a fractured lava. (At the time of the testing, fractured cores from the saturated zone near Yucca Mountain were not readily available.) Testing in the lava core was conducted at several different flow rates/residence times.

Details of the test procedures and the test results associated with the fractured volcanic core experiments are contained in Anghel (2001), so they are only summarized here. Tables 3 through 5 provide information on the fractured cores, and Table 6 gives the major ion chemistry of the U-20WW water used in the fractured core experiments. Besides their differences in surface characteristics, the silica colloids should have had greater diffusivity than the CML

microspheres by a factor of about 3.3 because of their smaller size, and they also should have settled about 2.75 times faster than the CML microspheres because of their greater density. The two cores differed significantly in their matrix porosities, with one having a relatively high porosity and the other having a very low one. One experiment was conducted in the higher porosity core (ER-20-6 #1, 2406 ft below surface). Four experiments were conducted in the lower porosity core. Test details for each experiment are provided in Table 7. In addition to the colloid tracers, each experiment also included iodide ion as a conservative (nonsorbing) solute tracer. The responses of the colloid tracers could thus be compared to that of a conservative solute to allow better quantification of any colloid retardation or early arrival. All tracers were injected simultaneously so that they would have exactly the same injection input function. The iodide was analyzed by ion-selective electrode, the silica spheres by high-sensitivity liquid in-situ particle spectrometry (HSLIS-S50, Particle Measuring Systems, Inc.), and the fluorescent microspheres by fluorometry.

Table 3. Properties of the Fractured Cores Used in the Colloid Transport Experiments: Physical Characteristics

Fracture (ft below land surface)	Fracture Length (cm)	Fracture Width (cm)	Matrix Porosity
PM-2, 7032 ft	14	9	0.014
ER-20-6#1, 2406 ft	23.8	12.7	0.369

Table 4. Properties of the Fractured Cores Used in the Colloid Transport Experiments: X-ray Diffraction Results (wt %)

Fracture	Smec-tite	Zeo-lite	Opal	Quartz	K-Spar	Plagio-clase	Hematite	Biotite	Calcite	Chlorite	Epidote/Clinzoisite	Total
PM-2 7032 ft	—	—	—	22.1	18.8	38.3	—	2.0	1.2	6.7	9.6	98.7
ER-20-6#1 2406 ft	1.7	83.4	27.3	0.9	4.8	3.3	—	1.5	—	—	—	102.7

NOTE: — = not detected

Table 5. Properties of the Fractured Cores Used in the Colloid Transport Experiments: Lithologic Descriptions

Fracture	Description
PM-2 7032 ft	Devitrified intermediate composition lava from the andesite of Mt. Helen of the Volcanics of Quartz Mountain.
ER-20-6#1 2406 ft	Highly zeolitic, poor to moderately-welded vitric, lithic tuff from the Calico Hills Formation.

Table 6. Chemical Composition of U-20WW Groundwater

Constituent	Concentration (mg/L)
Ca ²⁺	7.18 ± 0.05
K ⁺	1.3 ± 0.1
Na ⁺	60 ± 0.3
SiO ₂	46.9
Cl ⁻	11.6 ± 0
F ⁻	2.6 ± 0
HCO ₃ ⁻	110
SO ₄ ²⁻	32
pH	7.96
Specific Conductance (μS/cm)	296
TDS (mg/L)	273.8

Table 7. Summary of Experimental Conditions in the Fractured Core Tests

ER-20-6#1, 2406 ft

Flow Rate (mL/hr)	4.96
Fracture Orientation	Vertical
Injection Duration (hr)	10.0
Injection Concentration ⁽¹⁾	127 mg/L (I ⁻) 4.22 x 10 ⁷ particles/mL (0.33-µm yellow-green microspheres) 5.2 x 10 ¹⁰ particles/ml (0.1-µm silica)
Tracer Recoveries (Fractional)	0.85 (I ⁻) 0.63 (yellow-green microspheres) 0.72 (silica)

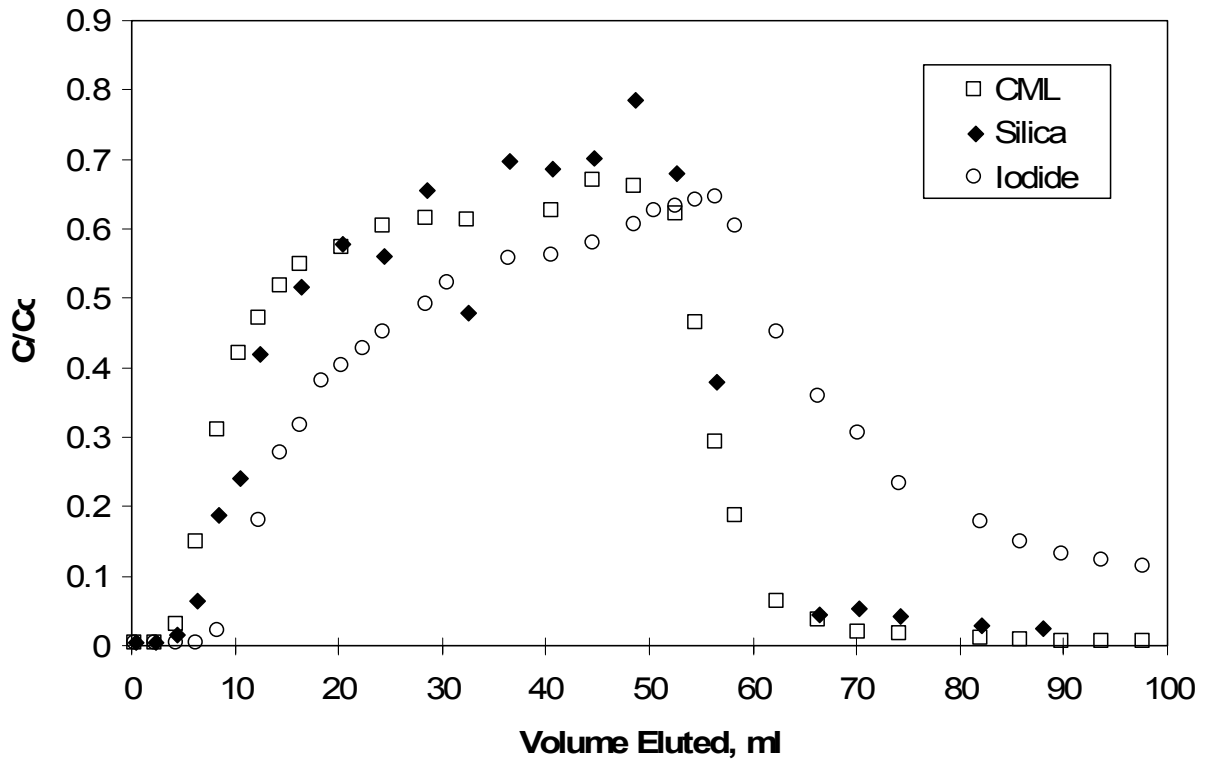
PM-2, 7032 ft

Experiment Number	1	2
Flow Rate (mL/hr)	10.02	2.5
Fracture Orientation	Vertical	Vertical
Injection Duration (hr)	3.3	13.2
Injection Concentration ⁽¹⁾	127 mg/L (I ⁻) 1.6 x 10 ⁷ particles/mL (0.33-µm yellow-green microspheres) 6.9 x 10 ¹⁰ particles/mL (0.1-µm silica)	127 mg/L (I ⁻) 1.9 x 10 ⁷ particles/mL (0.33-µm yellow-green microspheres) 7.9 x 10 ¹⁰ particles/mL (0.1-µm silica)
Tracer Recoveries (Fractional)	1.09 (I ⁻) 1.09 (yellow-green microspheres) 1.06 (silica)	1.06 (I ⁻) 0.89 (yellow-green microspheres) 0.88 (silica)
Experiment Number	3	4
Flow Rate (mL/hr)	0.58	0.57
Fracture Orientation	Vertical	Horizontal
Injection Duration (hr)	56	56
Injection Concentration ⁽¹⁾	127 mg/L (I ⁻) 1.9 x 10 ⁷ particles/mL (0.33-µm yellow-green microspheres) 7.4 x 10 ¹⁰ particles/L (0.1-µm silica)	127 mg/l (I ⁻) 1.7 x 10 ⁷ particles/mL (0.33-µm yellow-green microspheres) 7.5 x 10 ¹⁰ particles/mL (0.1-µm silica)
Tracer Recoveries (Fractional)	0.96 (I ⁻) 0.77 (yellow-green microspheres) 0.60 (Silica)	0.93 (I ⁻) 0.77 (yellow-green microspheres) 0.24 (Silica)

NOTE: ⁽¹⁾ Calculated concentrations for microspheres are as much as 20–30% of error. However, the normalized concentrations should be accurate to within 5%.

Figures 1 through 5 show the responses of each of the tracers in each of the five fractured core experiments. It is clear that at higher flow rates and shorter residence times, the CML microspheres and the silica spheres transported almost identically, with minimal attenuation of either colloid. However, both colloid tracers became more attenuated at lower flow rates, with the CML microspheres being consistently less attenuated than the silica spheres. It is also apparent from Figures 4 and 5 that the silica spheres were more attenuated in the horizontal orientation of the low-porosity fracture than in the vertical orientation at the same flow rate. In this case, a horizontal orientation means that the fractured core was oriented such that the fracture surfaces were parallel to the lab benchtop, whereas a vertical orientation means that the core was stood up on one of its ends with flow from bottom to top.

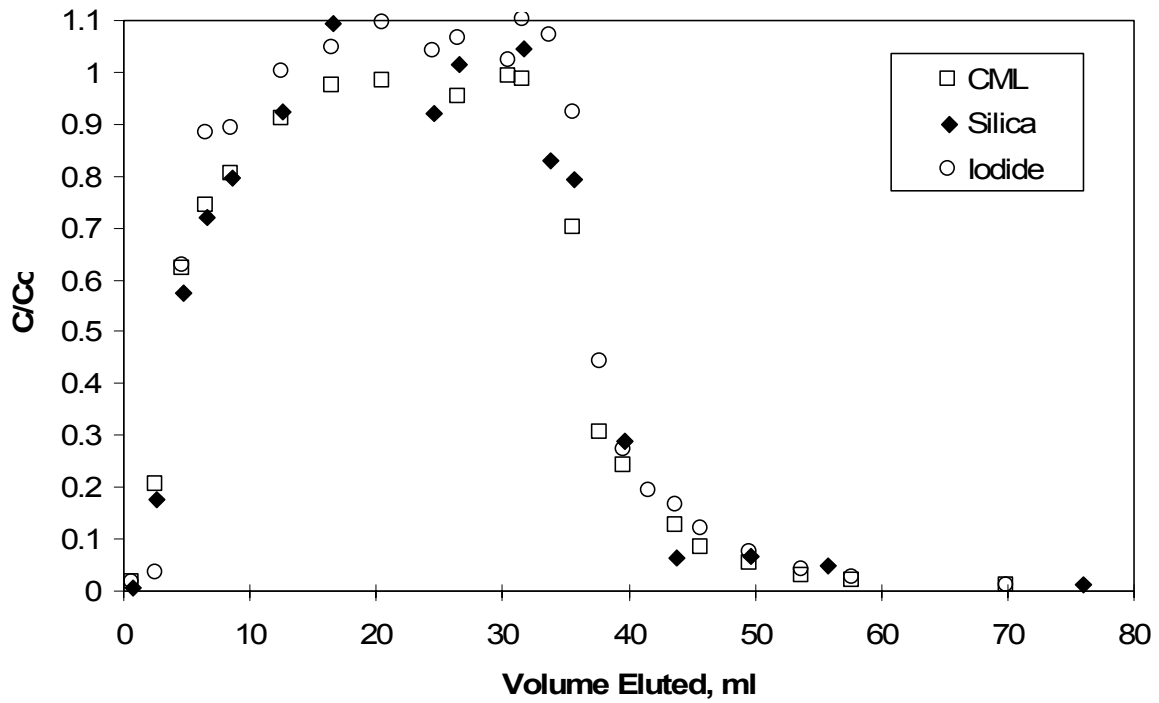
Quantitative interpretation of the tests in the lower-porosity fracture were carried out by Anghel (2001) using the RELAP computer model. The interpretive method involved first simultaneously fitting the iodide responses at each of the three flow rates through the core. The simultaneous fits yielded mean residence times, Peclet numbers, and matrix diffusion mass-transfer coefficients for the iodide in the core. The mean residence times for iodide were then assumed to apply to the colloid tracers, and the Peclet number and filtration coefficient (forward only) were allowed to vary to obtain a fit to the colloid response curves. The matrix diffusion mass-transfer coefficients for the colloid tracers were assumed to be zero. The resulting fitted parameter values are listed in Table 8. The single test in the higher-porosity fracture was only qualitatively interpreted because a single test at a constant flow rate does not allow unambiguous estimation of solute or colloid transport parameters. However, it is clear from Figure 1 that there was no significant difference in the transport of the two colloid tracers in this fracture. Also, the iodide appeared to experience a significant amount of matrix diffusion in this fracture based on its attenuated peak normalized concentration relative to the colloids and its extended tailing behavior. Colloid recoveries in this fracture suggested a colloid-filtration rate constant of $\sim 0.2 \text{ hr}^{-1}$.



NOTES: Flow rate was ~5 mL/hr, and the tracer injection pulse was ~50 mL.

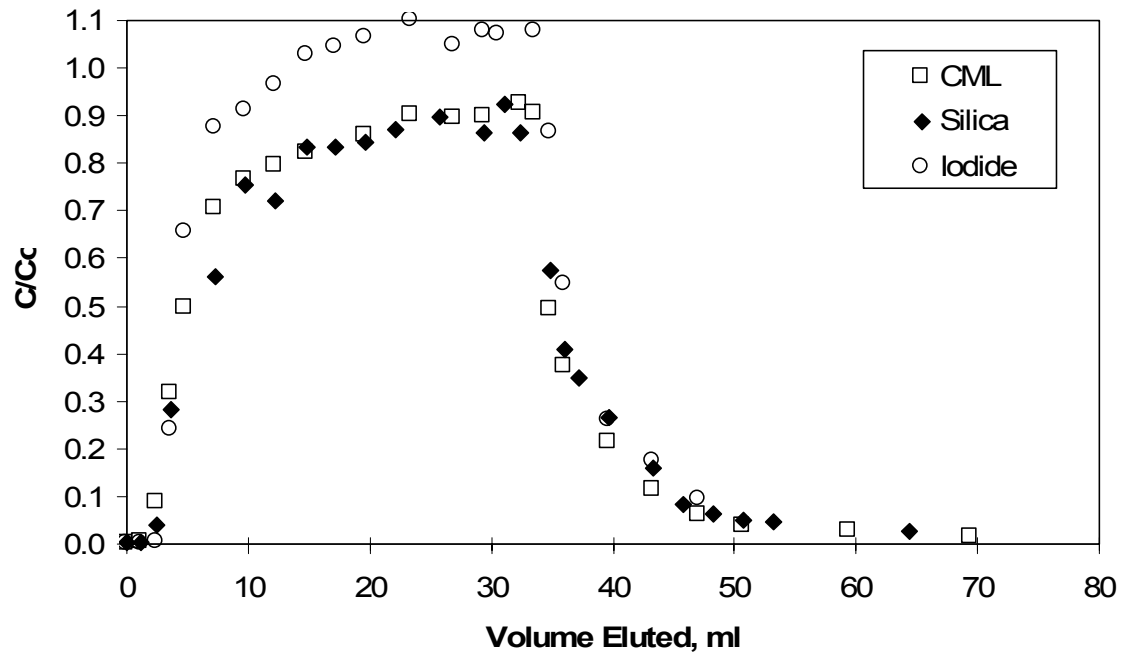
Normalized concentrations of silica less than about 0.03 in this figure and all other figures are subject to considerable error because background colloid concentrations begin to approach silica concentrations at these levels.

Figure 1. Normalized Concentrations of 330-nm Diameter CML Microspheres, 100-nm Diameter Silica Spheres, and Iodide in Fractured Core from ER-20-6#1 at 2407 ft



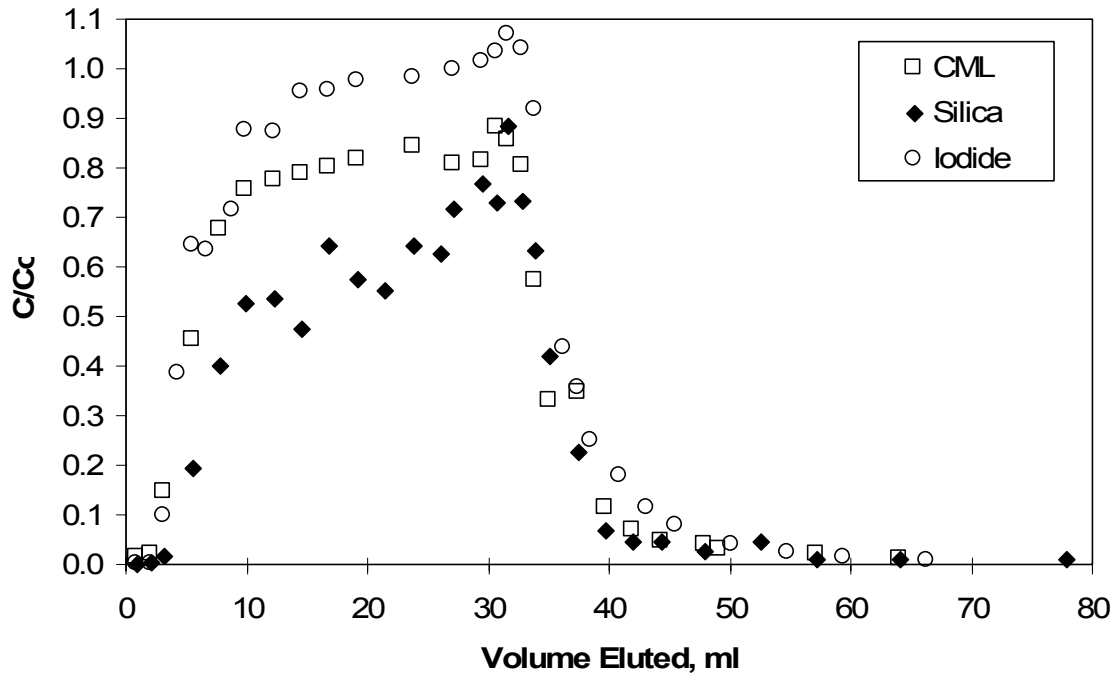
NOTES: Flow rate was ~10 mL/hr, with a mean tracer residence time of ~0.6 hr. The tracer injection pulse was ~33 mL.

Figure 2. Normalized Concentrations of 330-nm Diameter CML Microspheres, 100-nm Diameter Silica Spheres, and Iodide in Fractured Core from PM-2 at 7032 ft @10mL/hr



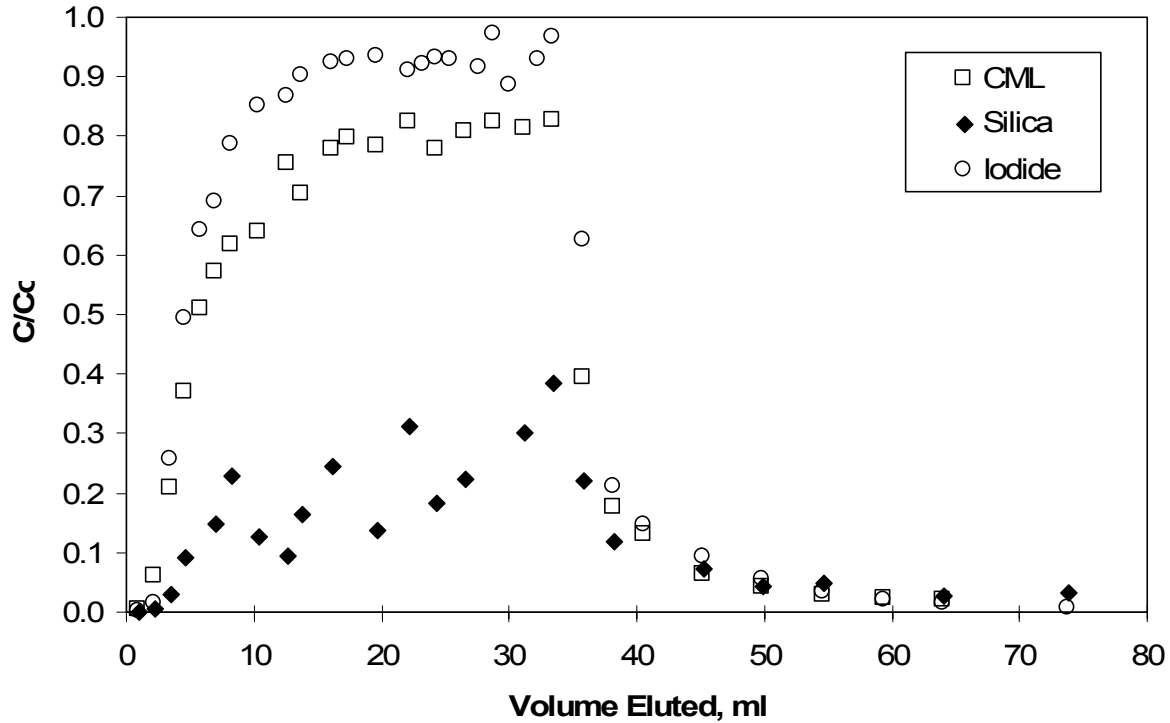
NOTES: Flow rate was ~2.5 mL/hr, with a mean tracer residence time of ~2.4 hr. The tracer injection pulse was ~33 mL.

Figure 3. Normalized Concentrations of 330-nm Diameter CML Microspheres, 100-nm Diameter Silica Spheres, and Iodide in Fractured Core from PM-2 at 7032 ft @2.5 mL/hr



NOTES: Flow rate was ~0.6 mL/hr, with a mean tracer residence time of ~10.4 hr. The tracer injection pulse was ~33 mL, and the orientation of the core was vertical.

Figure 4. Normalized Concentrations of 330-nm Diameter CML Microspheres, 100-nm Diameter Silica Spheres, and Iodide in Fractured Core from PM-2 at 7032 ft, Vertical Core Orientation



NOTES: Flow rate was ~0.6 mL/hr, with a mean tracer residence time of ~10.3 hr. The tracer injection pulse was ~33 mL, and the orientation of the core was horizontal.

Figure 5. Normalized Concentrations of 330-nm Diameter CML Microspheres, 100-nm Diameter Silica Spheres, and Iodide in Fractured Core from PM-2 at 7032 ft, Horizontal Core Orientation

Table 8. Model Parameters from RELAP Fits of Tracer Breakthrough Curves in Experiments in Fractured Core from Borehole PM-2

Model Parameter	Flow Rate (mL/hr)			
	10	2.5	0.6 (V)	0.6 (H)
Mean Fluid Residence Time (hr)	0.60	2.43	10.43	10.27
Half Aperture (cm)	0.024	0.024	0.024	0.024
Iodide Peclet Number	14	9.5	9.5	9.5
Iodide Dispersivity (cm)	1.0	1.5	1.5	1.5
Colloid Peclet Number	2.88	2.88	2.88	2.88
Colloid Dispersivity (cm)	4.86	4.86	4.86	4.86
Iodide Matrix Diffusion Coefficient (cm ² /s x 10 ⁷)	5.9	14.4	14.4	14.4
Microsphere Filtration Rate Constant (hr ⁻¹)	0.080	0.065	0.021	0.026
Silica Filtration Rate Constant (hr ⁻¹)	0.090	0.085	0.051	0.201

NOTE: V = vertical orientation; H = horizontal orientation.

Before drawing conclusions from the results of the fracture transport experiments, it is useful to define two characteristic length quantities:

$$L_D = \sqrt{2D\tau} \quad (\text{Eq. 1})$$

$$L_S = \left(\frac{1}{18\mu} \right) (\rho_p - \rho_f) g d_p^2 \tau = V_S \tau \quad (\text{Eq. 2})$$

where

L_D = characteristic diffusion distance during time τ , cm

L_S = characteristic gravitational settling distance during time τ , cm

D = colloid diffusion coefficient, cm^2/s

τ = residence time in fracture, s

V_S = settling velocity, cm/s

μ = fluid viscosity, $\text{g}/\text{cm}\cdot\text{sec}$

ρ_p = particle density, g/cm^3

ρ_f = fluid density, g/cm^3

g = gravitational acceleration, cm/s^2

d_p = particle diameter, cm.

The characteristic lengths L_D and L_S differed for the two colloid tracers in each of the fracture transport tests in the lower porosity fracture (Table 9).

Table 9. Characteristic Diffusion and Settling Lengths (L_D and L_S) for the CML Microspheres and Silica Spheres in the Four Experiments in the Fractured Core from Borehole PM-2

Characteristic Length	Flow Rate (mL/hr)			
	10	2.5	0.6 (V)	0.6 (H)
CML Diffusion Length, L_D (cm)	0.008	0.015	0.032	0.032
Silica Diffusion Length, L_D (cm)	0.014	0.028	0.058	0.057
CML Settling Length, L_S (cm)	0.0007	0.0028	0.012	0.012
Silica Settling Length, L_S (cm)	0.0019	0.0078	0.034	0.033

NOTES: The average fracture aperture ($2b$) was estimated to be 0.048 cm.

V = vertical orientation; H = horizontal orientation.

With these quantities defined, the following conclusions from the experiments can now be stated.

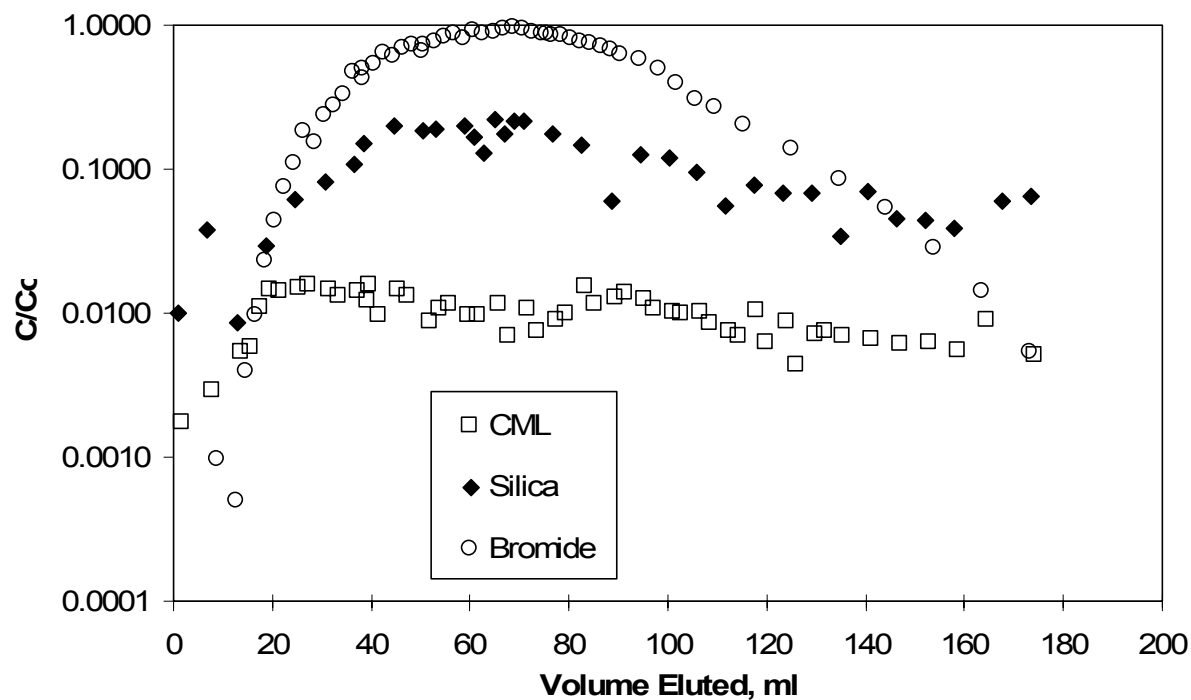
- When the fractures were in the vertical orientation, similar colloid responses were obtained at the same flow rate/residence time provided that $L_D/2b < 1$ for both colloids, where $2b =$ average fracture aperture ($b =$ half aperture). At flow rates where $L_D/2b > 1$ for the silica and $L_D/2b < 1$ for the CML microspheres, the latter transported with much less attenuation than the former.
- The fracture orientation influenced only the silica colloid transport, which is consistent with the greater silica settling velocity and the fact that $L_D/2b \approx 1$ for the silica spheres and $L_D/2b < 1$ for the CML microspheres. A significant fraction of the silica spheres were apparently able to settle to the lower surface of the horizontally oriented fracture during their residence time in the flow system, whereas most of the CML microspheres did not settle during this time.
- The “sticking efficiencies” (fractions of colloid-wall collisions that resulted in attachment) of the two colloids appeared to be quite similar. This conclusion is based on comparing the experimental results to colloid deposition theory in a parallel-plate channel in the absence of gravitational effects, which predicts that the filtration rate constant, k_f , should be proportional to $(\tau d_p^2)^{-1/3}$ if all colloid-wall collisions result in irreversible attachment (van de Ven 1989). The quantity d_p^2 for the CML microspheres was 10.9 times greater than that for the silica spheres, so the two colloids would be predicted to have the same k_f values when the residence time τ of the CML spheres is 10.9 times less than that for the silica. In fact, when the residence time was approximately 9 times less for the CML spheres, the filtration rates constants were 0.06 and 0.051 hr^{-1} for the CML and silica spheres, respectively. These rate constants are in relatively good agreement with each other (within experimental error), which suggests that the “sticking efficiencies” of the two colloids were very similar. Note that the CML rate constant of 0.06 hr^{-1} was obtained in an experiment conducted at a flow rate of approximately 5 ml/hr in which only CML microspheres and iodide were used as tracers. This experiment is not presented or discussed elsewhere in this report because it did not involve a direct comparison of CML microspheres and silica (all other experiments involved simultaneous injection of both colloid tracers). For details of the experiment, see Anghel (2001).
- The above three conclusions suggest that CML microspheres on the order of 250 to 500 nm in diameter should transport either very similarly to or conservatively relative to natural inorganic groundwater colloids in saturated fractured systems.

1.2 CML MICROSPHERE AND SILICA TRANSPORT IN SATURATED ALLUVIUM

Column experiments were conducted in two separate 30-cm long by 2.5-cm diameter glass columns equipped with PTFE end fittings, including a 20- μm end frit and PTFE tubing. The alluvium used in the experiments was obtained from NC-EWDP-19D1 at the depth intervals of 405 to 410 and 420 to 425 ft below ground surface, approximately 50 to 75 ft below the water table. Cuttings samples were wet sieved (using NC-EWDP-19D1 well water) in the laboratory

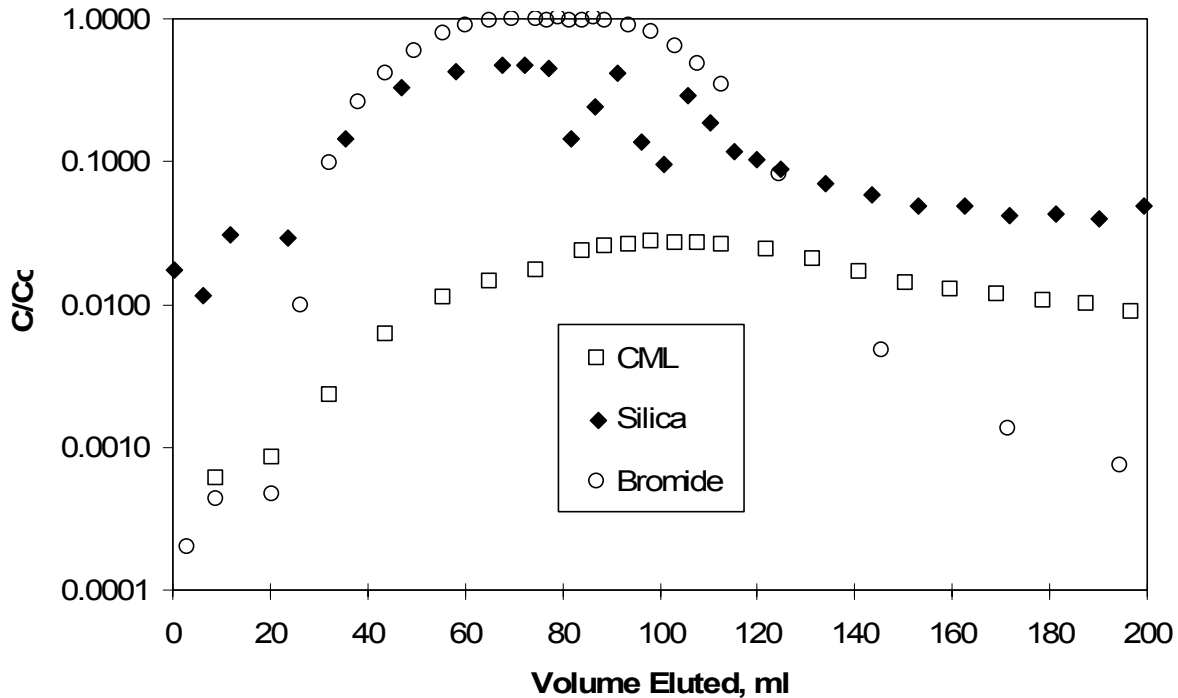
(ASTM 1998), and the size range between 75 and 2000 μm was retained for testing. Material from the two intervals was combined in a 50:50 mass ratio for the column experiments because there was not enough material from the individual intervals to pack the columns. The water used in testing was taken from the uppermost screened interval of well NC-EWDP-19D1.

The CML microsphere and silica transport experiments in alluvium-packed columns were conducted in the same columns in which the lithium bromide column studies were conducted. The water used in testing was taken from the uppermost screened interval of well NC-EWDP-19D1. The column experiments involved the simultaneous introduction of the same 330-nm-diameter CML microspheres and 100-nm-diameter silica spheres used in the fracture experiments along with sodium bromide, with bromide ion serving as a nonsorbing solute tracer. Bromide was analyzed by ion chromatography. The first two experiments were conducted at flow rates of 2 and 6 mL/hr in Columns A and B, respectively. The normalized concentration responses of the colloids and bromide in these two experiments are shown in Figures 6 and 7. Not surprisingly, the normalized concentrations and recoveries of both colloid tracers were greater in the column with the higher flow rate (Column B). However, in contrast to the fracture transport experiments, the CML microspheres were more attenuated than the silica spheres in both columns. The greater attenuation of the CML microspheres relative to the silica spheres could be the result of enhanced deposition of the larger microspheres by inertial interception (collisions with alluvium grains as a result of inertial forces in the fluid flow). Inertial interception in a porous medium is predicted to be proportional to $(d_p/d)^2$ (Harvey and Garabedian 1991), where d_p is the colloid diameter and d is the grain size of the porous medium.



NOTE: The flow rate was ~2 mL/hr.

Figure 6. Log Normalized Concentrations of 330-nm Diameter CML Microspheres, 100-nm Diameter Silica Spheres, and Bromide in Alluvium-Packed Column A



NOTE: The flow rate was ~6 mL/hr.

Figure 7. Log Normalized Concentrations of 330-nm Diameter CML Microspheres, 100-nm Diameter Silica Spheres, and Bromide in Alluvium-Packed Column B

For the fracture transport experiments, colloid interception played an insignificant role in deposition because the average fracture aperture was on the order of 0.5 mm (i.e., very large compared to the colloid diameters) and the fracture walls were primarily parallel to flow. However, in a porous medium, flow can follow much more tortuous pathways around grains, and pore throats around small grains may be quite narrow. Although sieving of the material used to pack the columns was intended to exclude grain sizes smaller than 75 μm in diameter, it is likely that finer material was present in the columns or perhaps generated after the columns were allowed to flow. Also, because of the irregular shapes of the alluvium grains, most pore throats were probably quite a bit narrower than would be predicted assuming spherical grains. These factors may have resulted in a significant number of inertial collisions of the CML microspheres with the alluvium grains in the columns. The silica spheres, however, had a value of $(d_p/d)^2$ about a factor of 11 less than that of the CML microspheres, so inertial interception would be expected to play a much less important role in their deposition.

A second set of CML microsphere and silica-sphere transport experiments was conducted in the two alluvium-packed columns. The second experiment in Column B was conducted at the same flow rate as the first experiment in this column (~6 mL/hr), whereas the second experiment in Column A was conducted at a flow rate of ~12 mL/hr, approximately 6 times greater than in the first experiment. The normalized concentration responses of the tracers in these two experiments are shown in Figures 8 and 9. When comparing the first and second experiments in Column B

(Figures 7 and 9), it is apparent that both colloids were significantly more attenuated in the second experiment, and the CML microspheres became even more attenuated relative to the silica spheres. The recovery of the silica spheres decreased by about a factor of 3 in the second experiment, whereas the recovery of the CML microspheres decreased by nearly a factor of 10. These decreases might be attributed to a decrease in the hydraulic conductivity of the columns, which often occurs over time due to microbial growth or redistribution of fines, both of which tend to decrease effective pore throat diameters in columns. The hydraulic conductivity of both columns was measured only after the second test, not prior to either test, so it was not possible to unequivocally attribute the decrease in colloid recoveries in Column B to a decrease in hydraulic conductivity.

The second experiment in Column A was probably influenced by the presence of air pockets that appeared in both the top and bottom ends of the column some time after the first experiment had been completed. These air pockets were presumably the result of slow leaks that occurred in the top and bottom end fittings of the columns. Normally, one would expect a greater recovery of both colloid tracers at a significantly higher flow rate, but in this case, the CML microsphere recovery was only marginally higher than in the first test, and the silica sphere recovery was lower. Also, unlike the other three alluvium column tests, the microsphere recovery was higher than the silica recovery in this test. The lower-than-expected recoveries of both colloid tracers and the fact that the silica was more attenuated than the microspheres are tentatively attributed to the attachment of both colloids to the air-water interfaces present at either end of the column. It is well known that colloids that come into contact with air-water interfaces become essentially irreversibly attached to the interface as a result of strong capillary forces (Abdel-Fattah and El-Genk 1998). The silica spheres would be expected to collide more frequently with these interfaces than the CML microspheres because of their greater diffusivity, thus resulting in greater attenuation relative to the CML microspheres.

Table 10 provides preliminary estimates of filtration and detachment rate constants for the CML microspheres and silica in each of the alluvium column experiments. These estimates were obtained by fitting the experimental data using the same approach as described in Section 1.1 for estimating filtration rate constants in the fractured cores. That is, the RELAP model was used to fit the bromide responses to estimate the mean residence times and Peclet numbers in the column tests, and then the filtration and detachment rate constants were adjusted to fit the colloid responses. The detachment rate constants were constrained by fitting the tails of the colloid responses. It should be recognized that the detachment rate constants for silica are very crude estimates because the silica tails rapidly approached background colloid concentrations. Table 10 also provides the effective partition coefficients (K_d values) for the colloids in each experiment, given by the filtration rate constant divided by the detachment rate constant. These retardation factors would apply to large time scales if it is assumed that filtration is completely reversible.

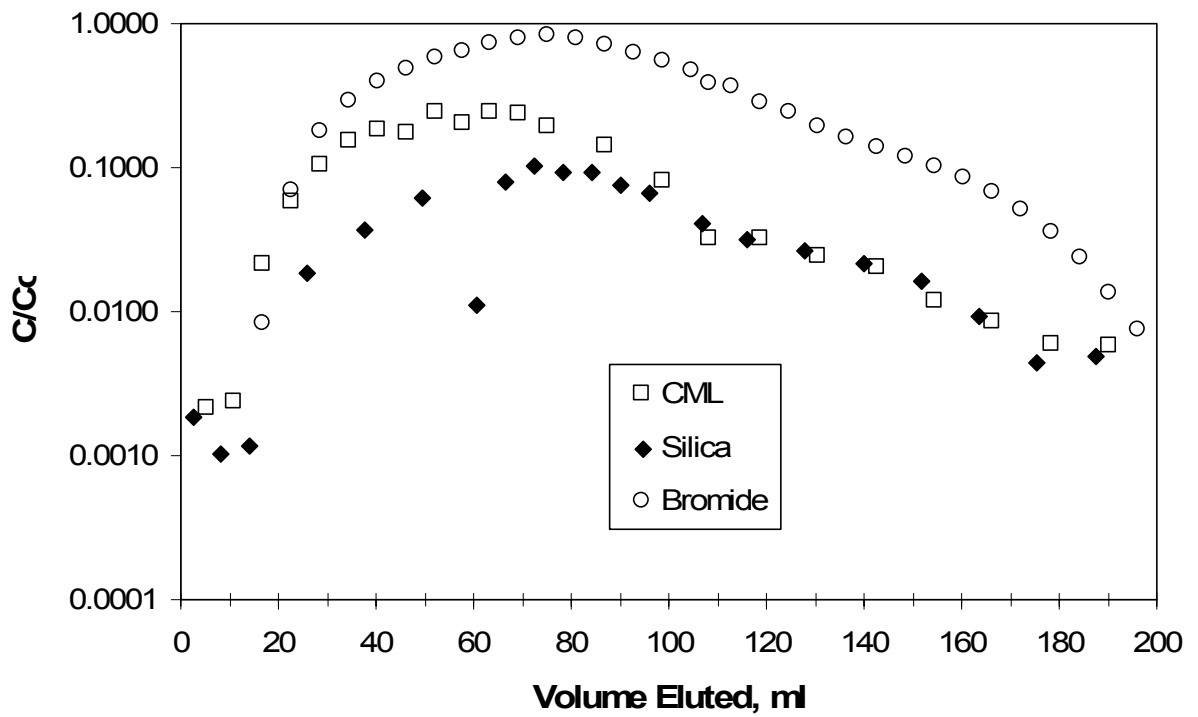
Table 10. Estimates of Filtration Rate Constants and Detachment Rate Constants for CML Microspheres and Silica Colloids in Columns Packed with Alluvium

Colloid Transport Parameters	Column / Flow Rate			
	A / 2 mL/hr	B / 6 mL/hr	A / 12 mL/hr	B / 6 mL/hr
CML filtration rate constant (hr^{-1})	0.68	0.6	0.38	0.91
CML detachment rate constant (g/ml-hr)	0.004	0.018	0.0027	0.0065
CML K_d value (ml/g)	170	33	140	140
Silica filtration rate constant (hr^{-1})	0.22	0.13	0.73	0.28
Silica detachment rate constant (g/ml-hr)	0.0022*	0.0076	0.0037	0.0147
Silica K_d value (ml/g)	100	17	200	19

*NOTE: This value cannot be practically distinguished from zero.

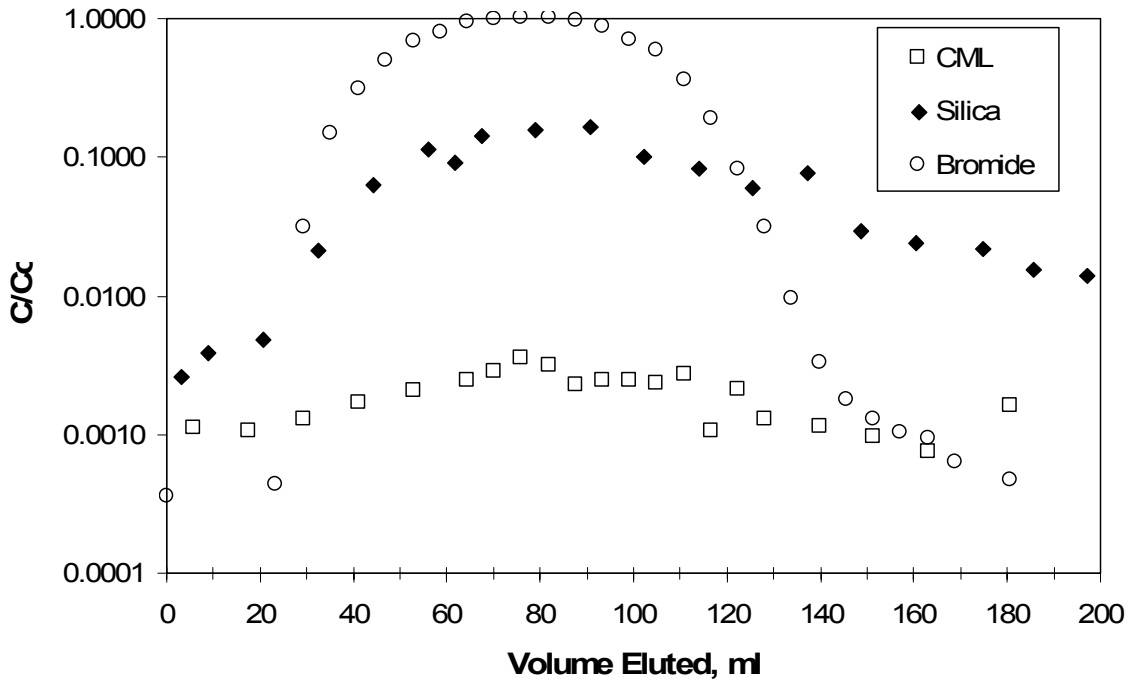
It is apparent from Figures 6 through 9 and Table 10 that the relative transport behavior of the CML microspheres and the silica spheres was significantly different in the alluvium columns from that in the fractured cores. These differences are tentatively attributed to smaller pore throat sizes in the alluvium columns and, hence, greater inertial interception of the CML microspheres in these columns. However, differences in the relative transport behavior of the two colloid tracers could also be the result of mineralogical differences or differences in the water chemistry in the two sets of tests. The results indicate that CML microspheres with diameters greater than ~300 nm will not necessarily behave as conservative surrogates for natural groundwater colloids in the saturated alluvium south of Yucca Mountain. However, Table 10 suggests that filtration rate constant estimates derived from CML microsphere responses in field tracer tests in alluvium could be divided by a factor of 3 to 5 to obtain reasonable estimates of filtration rate constants for inorganic colloids in saturated alluvium. Detachment rate constants for CML microspheres and silica in the laboratory column tests, though not well constrained, agreed within a factor of 2.5.

Results from field testing using microspheres will be used to validate the efficiency factors for the filtration analysis used to derive the retardation factors for the irreversible colloids. In the absence of further testing, one approach is to divide field-derived CML microsphere filtration rate constants by 5 and multiply microsphere detachment rate constants by 2.5 to obtain conservative estimates of inorganic colloid filtration and detachment rate constants in saturated alluvium.



NOTE: The flow rate was ~12 mL/hr.

Figure 8. Log Normalized Concentrations of 330-nm Diameter CML Microspheres, 100-nm Diameter Silica Spheres, and Bromide in Second Experiment in Alluvium-Packed Column A



NOTE: The flow rate was ~6 mL/hr.

Figure 9. Log Normalized Concentrations of 330-nm Diameter CML Microspheres, 100-nm Diameter Silica Spheres, and Bromide in Second Experiment in Alluvium-Packed Column B

2. CONCLUSIONS

Laboratory studies comparing CML microsphere and silica colloid transport in fractured volcanic rocks indicated that CML microspheres of approximately 300-nm diameter behaved as conservative surrogates for 100-nm silica colloids in fractured rock. That is, the CML microspheres transported with less attenuation than the silica colloids in the fractures. However, similar tests in columns packed with saturated alluvium indicated that 300-nm CML microspheres may not necessarily transport as conservative surrogates for silica colloids in saturated alluvium (the microspheres were more attenuated than the silica in 3 of 4 column experiments). The fact that the CML microspheres did not transport conservatively relative to silica in the alluvium column experiments does not negate their usefulness as colloid tracers in field tests. It simply means that the colloid transport parameters derived from field tracer testing with CML microspheres will have to be appropriately adjusted or corrected (perhaps through wider uncertainty bounds) before being used in validation of parameters used in performance assessment models. In the absence of further testing and analysis, one approach would be to divide field-derived CML microsphere filtration rate constants by 5 and multiply microsphere detachment rate constants by 2.5 to obtain conservative estimates of inorganic colloid filtration and detachment rate constants in saturated alluvium. This topic will be addressed in greater detail in a revision of the SZ Colloid-Facilitated Transport Analysis Report (CRWMS M&O 2000).

3. INPUTS AND REFERENCES

3.1 DOCUMENTS CITED

Abdel-Fattah, A.I. and El-Genk, M.S. 1998. "On Colloid Particle Sorption onto a Stagnant Air/Water Interface." *Advances in Colloid and Interface Science*, 78, 237–266. Amsterdam, The Netherlands: Elsevier.

Anghel, I. 2001. *Comparison of Polystyrene and Silica Colloids Transport in Saturated Rock Fractures*. M.S. Thesis. Albuquerque, New Mexico: University of New Mexico.

ASTM (American Society for Testing and Materials) 1998. *Annual Book of ASTM Standards. Section 4: Construction. Volume 04.08 Soil and Rock (I): D420 - D4914*. West Conshohocken, Pennsylvania: American Society of Testing and Materials.

Bales, R.C.; Gerba, C.P.; Grondin, G.H.; and Jensen S.L. 1989. "Bacteriophage Transport in Sandy Soil and Fractured Tuff." *Applied and Environmental Microbiology*, 55 (8), 2061–2067. Washington, D.C.: American Society for Microbiology.

CRWMS M&O (Civilian Radioactive Waste Management System Management and Operations). 2000. *Saturated Zone Colloid-Facilitated Transport*. ANL-NBS-HS-000031, REV 00. Las Vegas, Nevada: CRWMS M&O.

Harvey, R.W. and Garabedian, S.P. 1991. "Use of Colloid Filtration Theory in Modeling Movement of Bacteria through a Contaminated Sandy Aquifer." *Environmental Science and Technology*, 25, 178–185. Washington, D.C.: American Chemical Society.

Hiemenz, P.C. 1986. *Principles of Colloid and Surface Chemistry* (2nd ed.). New York, New York: Marcel Dekker, Inc.

Reimus, P.W.; Ware, S.D.; Lu, N.; Abdel-Fattah, A.I.; Kung, K.S.; and Neu, M.P. 2001. "FY 2001 Progress Report on Colloid-Facilitated Plutonium Transport in Fractured Rocks from Pahute Mesa, Nevada Test Site." *Underground Test Area Project Report*. Los Alamos, New Mexico: Los Alamos National Laboratory.

Steinkamp, J.A.; Habbersett, R.C.; and Hiebert, R.D. 1991. "Improved Multilaser/Multiparameter Flow Cytometer for Analysis and Sorting of Cells and Particles." *Review of Scientific Instruments*, 62 (11), 2751–2764. New York, New York: American Institute of Physics.

Wan, J. and Wilson, J.L. 1994. "Colloid Transport in Unsaturated Porous Media." *Water Resources Research*, 30 (4), 857–864. Washington, D.C.: American Geophysical Union.

3.2 CODES, STANDARDS, REGULATIONS, AND PROCEDURES

40 CFR 197. 2001. Protection of Environment: Public Health and Environmental Radiation Protection Standards for Yucca Mountain, Nevada.